

Communication

Synthesis and Characterization of a Binuclear Copper(II)-dipyriamethyrin Complex: $[\text{Cu}_2(\text{dipyriamethyrin})(\mu_2\text{-1,1-acetato})_2]$

James T. Brewster II ¹, Harrison D. Root ¹, Hadiqa Zafar ¹, Gregory D. Thiabaud ¹, Adam C. Sedgwick ¹, Jiaming He ², Vincent M. Lynch ¹ and Jonathan L. Sessler ^{1,*}

¹ Department of Chemistry, The University of Texas at Austin 105 E 24th Street-Stop A5300, Austin, TX 78712-1224, USA; jbrewste@utexas.edu (J.T.B.II); hroot@utexas.edu (H.D.R.); hzafar@mit.edu (H.Z.); gtamanaco@msn.com (G.D.T.); a.c.sedgwick@utexas.edu (A.C.S.); vmlynch@cm.utexas.edu (V.M.L.)

² Materials Science and Engineering Program and Texas Materials Institute, The University of Texas at Austin, Austin, TX 78712, USA; jiaminghe@utexas.edu

* Correspondence: sessler@cm.utexas.edu

Academic Editor: José A. S. Cavaleiro

Received: 3 March 2020; Accepted: 21 March 2020; Published: 23 March 2020



Abstract: The reaction between dipyriamethyrin and copper(II) acetate $[\text{Cu}(\text{OAc})_2]$ afforded what is, to our knowledge, the first transition metal-dipyriamethyrin complex. Molecular and electronic characterization of this binuclear Cu(II) complex via EPR, UV-vis, and single crystal X-ray diffraction analysis revealed marked differences between the present constructs and previously reported binuclear copper(II) hexaphyrin species. UV-vis titration analyses provided evidence for a homotropic positive allosteric effect, wherein the binuclear species is formed without significant intermediacy of a monomeric complex.

Keywords: dipyriamethyrin; expanded porphyrin; binuclear copper; porphyrinoid; allosteric effect

1. Introduction

The incorporation of specific metal ions within enzyme active sites facilitates numerous chemical transformations required for proper biological function [1–3]. Mutation of the amino acids defining the cation coordination sphere can lead to structural modification of the core metal complex geometry with concomitant loss or gain of function [4,5]. Non-native enzymatic systems, prepared by switching important amino acid residues or the coordinated metal ion, have provided mechanistic insights into the action of many metalloenzymes [6]. Concurrent with these efforts, non-natural and synthetic model systems have allowed for the controlled modulation of desired properties and provided access to new chemistry [7–11].

Tetrapyrrolic porphyrins and related congeners have found widespread utility as mononuclear metalloenzyme active site mimics with attendant applications in catalysis, among other uses [12–14]. Extension of these efforts to multiple metal and main group ion complexes remains rare. Indeed, only a few examples of binuclear complexes, such as Rh, Hg, Re, Tc, B, and alkali metal ions, have been structurally characterized [15–22]. Expanded porphyrinoids, frameworks containing a larger internal cavity, have extended the chemistry of such systems via the stabilization of multiple metal ions coordinated within a single lacuna [23,24]. Within this paradigm, expanded and related non-conjugated larger porphyrinoid systems have yielded a diverse array of homo- and hetero-binuclear transition metal and main group complexes [22,25–45]. Previous efforts by our group using hexaphyrin expanded porphyrins have also resulted in the synthesis and characterization of binuclear copper complexes (Figure 1) [18,46–48]. In these instances, modification of the heterocyclic components within the hexaphyrin core has allowed for subtle changes in the electronic structure and metal-metal communication.

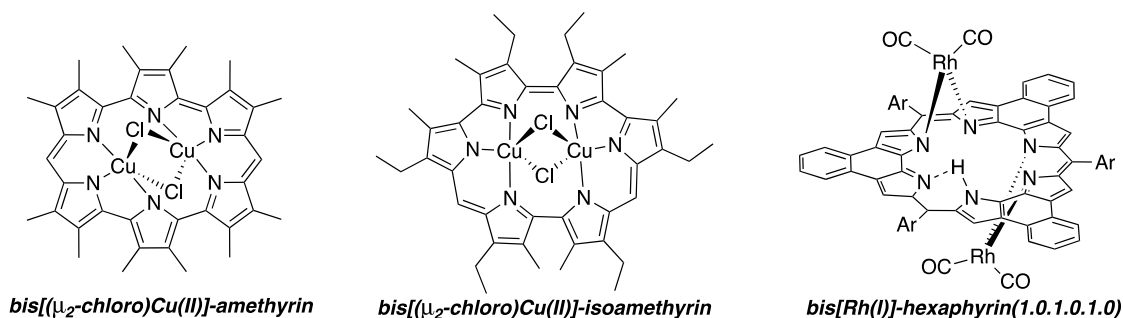
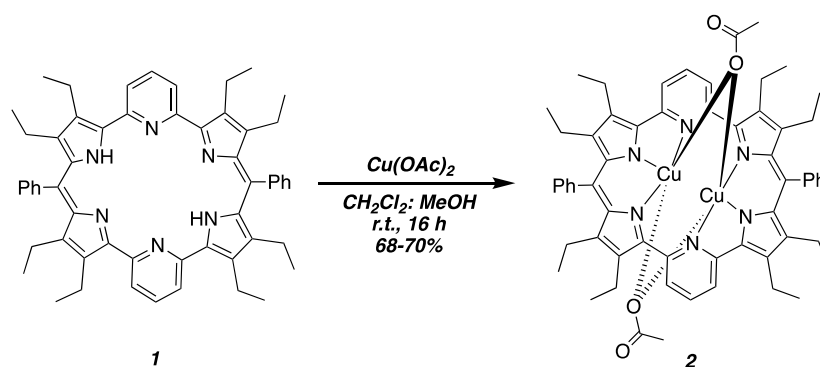


Figure 1. Representative binuclear hexaphyrin complexes.

Recent efforts with the so-called dipyriamethyrin ligand (**1**), a bis-pyridine hexaaza-porphyrinoid, yielded a series of thorium(IV), uranium(IV), neptunium(IV), and uranyl(VI) complexes [49,50]. However, transition metal complexes have yet to be reported using this hexaphyrin analogue. We envisaged that the mixed heterocyclic coordinating motifs present in dipyriamethyrin **1** might confer new properties to a transition metal complex distinct from previous hexaphyrin species. Here, we report the synthesis and characterization of a binuclear [Cu₂(dipyriamethyrin)(μ_2 -1,1-acetato)₂] complex (**2**). The molecular and electronic properties of **2** were characterized by UV-vis and EPR spectroscopy, cyclic voltammetry, and single crystal X-ray diffraction analysis.

2. Results and Discussion

The dipyriamethyrin of this study was prepared using our recently optimized procedure [50]. Treatment of the free-base form of **1** with copper acetate [Cu(OAc)₂] (25 equiv.) in a methanol:dichloromethane mixture (1:1, *v/v*) open to the laboratory atmosphere at room temperature for 16 h yielded the dinuclear copper complex **2** as a purple solid with green metallic lustre in 68–70% yield, after purification by filtration over Celite and crystallization from dichloromethane: hexanes (Scheme 1 & ESI Figure S1). The purified complex **2** proved unstable under prolonged exposure of protic and non-anhydrous solvents, reverting back to the free-base ligand (**1**) or a mixture of complex **2** and ligand **1**, respectively. Complex **2** also proved unstable under conditions of silica gel, neutral aluminum oxide, and basic aluminium oxide purification. However, **2** proved sufficiently stable in neutral, apolar media to allow for characterization, including via single crystal X-ray diffraction analysis. Interestingly, the equilibrium between metallation and protonation observed with complex **2** was not seen with related amethyrin and (naphtho)isoamethyrin species [46–48]. In the case of previous hexaphyrin ligands, formation of the binuclear Cu(II) complex was believed to occur with a concomitant 2 π -electron oxidation yielding a globally aromatic porphyrinoid ligand. No such redox chemistry was observed in the case of dipyriamethyrin and may contribute to the metal complex lability.



Scheme 1. Synthesis of binuclear copper(II) complex **2**.

Upon metalation, an easy-to-visualize solution-state colour change from yellow-orange to pink-purple was observed (Figure 2a). The UV-vis spectral profile, as measured in tetrahydrofuran, displayed a slight decrease in the molar absorptivity from $\epsilon = 46600 \text{ M}^{-1} \text{ cm}^{-1}$ to $\epsilon = 32900 \text{ M}^{-1} \text{ cm}^{-1}$ with a bathochromic shift in the Soret-band ($\lambda_{\text{max}} = 539 \text{ nm}$). Dipyrriamethyrin (**1**) is not fully through conjugated, i.e., globally aromatic. In terms of its electronic features, it thus behaves more similar to dipyrromethene with the major transition ($\lambda_{\text{max}} = 466$) being assigned as a charge transfer process associated with the π -system of the dipyririn subunit [51–53]. The large absorption in dipyrriamethyrin (**1**) and the binuclear copper complex (**2**) are attributed to the dipyrriamethyrin π - π^* transition [54]. Previous studies on transition metal complexes also report a bathochromic shift to the λ_{max} , suggesting a metal-mediated reduction in the HOMO-LUMO gap [52–55]. Furthermore, in analogy to studies on Th(IV), U(IV), and Np(IV)-dipyrriamethyrin complexes, the broadening of the Soret-like band in complex **2** may be due to an overlapping metal-to-ligand charge transfer (MLCT) transition [50]. UV-vis titration analysis using dipyrriamethyrin ($9.4 \mu\text{M}$) in THF and $\text{Cu}(\text{OAc})_2$ (0.33 mM stock solution in THF) showed direct conversion from the free-base **1** to the binuclear Cu(II) complex **2** (Figure 2b,c). Formation of **2** is posited to arise via the intermediacy of a sitting atop (SAT) complex followed by a homotropic positive allosteric process wherein the first cation complexation event serves to activate the dipyrriamethyrin ring for the second binding event [20,55–60]. Evidence for a potential positive allosteric (i.e., acetate directing) effect was also gleaned from X-ray crystallographic data (ESI Figure S2). Formation of the initial mono-metallated complex is postulated to arise through cooperation between the Cu(II) cation and acetate counter by a concerted metalation-deprotonation (CMD)-type mechanism (cf. ESI, Scheme 1) [61–63].

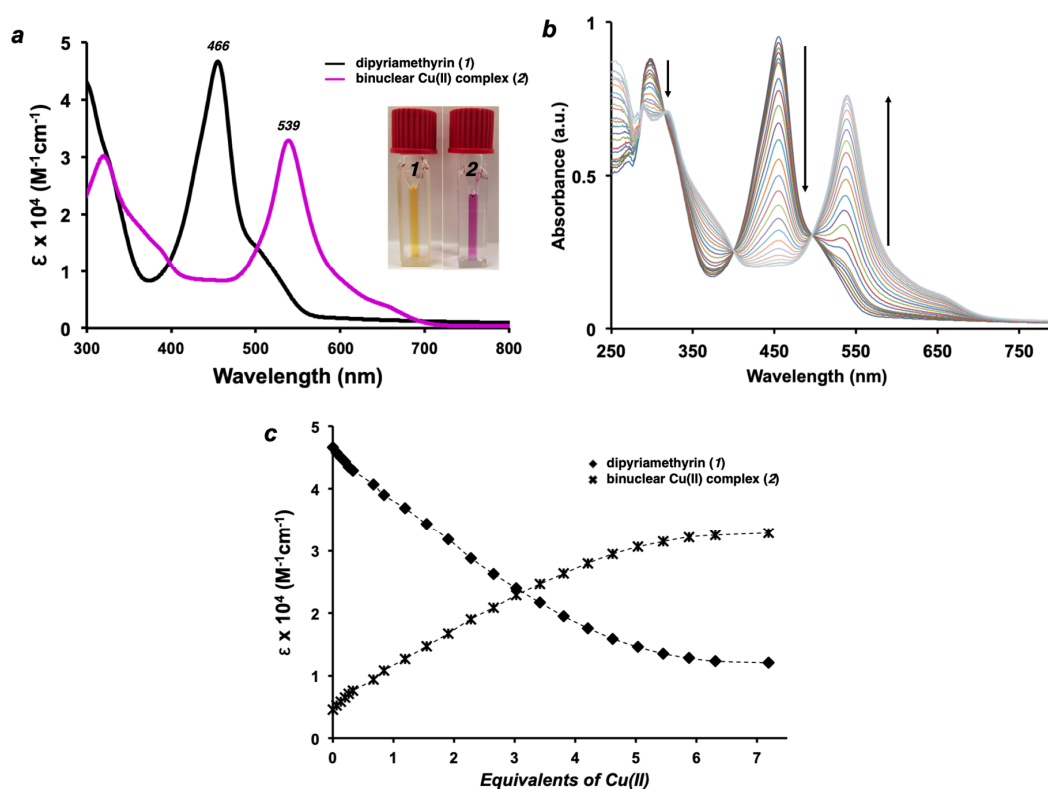


Figure 2. (a) UV-vis spectrum of ligand **1** (black) and complex **2** (pink) in THF. The insert shows photographs of **1** and **2** as solutions in tetrahydrofuran. (b) UV-vis titration data corresponding to the conversion of the free-base dipyrriamethyrin **1** ($9.4 \mu\text{M}$) to the corresponding binuclear Cu(II) complex **2** upon the addition of $\text{Cu}(\text{II})(\text{OAc})_2$ in THF and (c) changes in the molar absorptivity (ϵ) at the maximum wavelength (λ_{max} of **1** = 466 nm; λ_{max} of **2** = 539 nm) plotted against equivalents of $\text{Cu}(\text{II})(\text{OAc})_2$.

Crystals suitable for X-ray diffraction analysis were grown via evaporation of a dichloromethane:hexanes (1:2, *v/v*) solution of **2**. As illustrated in Figure 3, the binuclear copper complex (**2**) adopts a twisted conformation so as to complex the two Cu(II) ions effectively. Torsion within the porphyrinoid ring arises from a twist between the biaryl (C_{sp^2} - C_{sp^2}) pyridine-pyrrole heterocyclic subunits (i.e., N1 to N2 and N4 to N5). In analogy to previous binuclear Cu(II)-amethyrin complexes, all six heterocycles participate in coordination to the complexed metal ions. The coordination environment of Cu1 is defined by an equatorial pyrrol-2-ylidene (N6) and 1,1-acetates (O1 and O2) with additional axial pyridine (N1) and pyrrole (N5) donors. A similar first coordination sphere is found for Cu2 with N3, O1, and O2 defining the equatorial plane and N2 and N4 defining the axial plane.

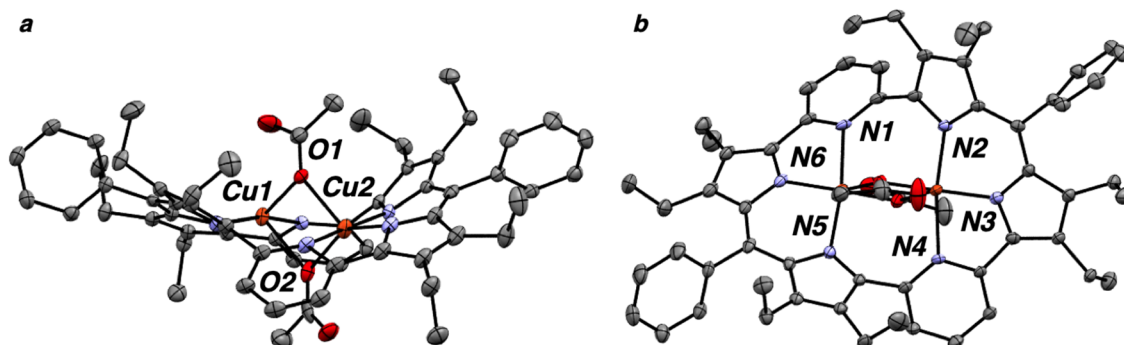


Figure 3. Single crystal X-ray structures of complex **2** viewed from (a) side and (b) top perspective. Hydrogen atoms are omitted for clarity.

Following the approach of Addison and co-workers, wherein the structural parameter τ_5 is calculated as an index of trigonality with $\tau_5 = 1$ being defined as an ideal trigonal bipyramidal geometry [64], the bis-copper(II) complex **2** is characterized by $\tau_5 = 0.69$ for Cu1 and 0.73 for Cu2, respectively [65]. These values represent a lower level of distortion than related amethyrin species, a finding attributed to the enhanced flexibility of the dipyriamethyrin core [50]. The nitrogen-Cu(II) distances reveal an asymmetric coordination environment and are 2.107(2) Å (N1-Cu1), 1.987(3) Å (N2-Cu2), 1.889(2) Å (N3-Cu2), 2.080(2) Å (N4-Cu2), 1.998(2) Å (N5-Cu1), and 1.867(2) Å (N6-Cu1), respectively. The Cu(II)-Cu(II) distance, 3.0276(6) Å, is longer than that found in the case of the corresponding complexes of amethyrin (2.761(1) Å), isoamethyrin (2.744(2) Å), and naphthoisoamethyrin (2.752 Å). Unlike the binuclear Cu(II) complex of amethyrin, the core structure of **2** contains bridging acetates. The four Cu-O bond distances are nonequivalent at 1.971(4) Å (O1-Cu1) and 2.181(4) Å (O1-Cu2) and 2.134(2) Å (O2-Cu1) and 1.968(2) Å (O2-Cu2). The bond angles (θ) of the μ_2 -1,1-acetates are 93.36° for Cu1-O1-Cu2 and 94.90° for Cu1-O2-Cu2, respectively. Single crystal X-ray crystallographic analysis of the binuclear copper(II)-dipyriamethyrin system also revealed a mixture of μ_2 -acetate and μ_2 -chloride anions bound to the Cu(II) ions. The site occupancy factor for the chloride ion refined to 11%. Similar acetate-chloride ligand exchange has been seen with the related isoamethyrin and naphthoisoamethyrin binuclear copper(II) complexes [47,48]. Attempts to prevent ligand exchange by using different solvent systems (i.e., THF, THF:hexanes, toluene, and toluene:hexanes) failed to yield X-ray diffraction grade single crystals. Attempts to convert **2** from the partial bis-bridging acetate complex to the fully bis-bridging chloride species (i.e., by prolonged solvation in CH_2Cl_2 exposed to light) also failed to yield X-ray quality single crystals.

EPR spectroscopic studies using freshly prepared complex **2**, carried out at 100 K in frozen toluene, revealed features readily assignable to two coupled copper(II) ions [66]. The spectrum of **2** yielded an EPR pattern for the triplet state ($S = 1$) with both $\Delta M_s \pm 1$ and $\Delta M_s \pm 2$ (half-field transition; $g = 4.15$) features being observed (Figure 4). This is consistent with a pair of copper(II) ions. To probe the putative electronic exchange between the copper ions, analogous studies were carried out at 300 K in toluene solution. In this case, the signal intensity decreased significantly and was devoid of discernible signals. Presumably, this reflects a lower level of coupling under these latter higher temperature

conditions. Similar temperature dependence was seen with amethyrin and naphthoisoamethyrin, as well as simpler fused and monomeric porphyrin constructs [46,48,67,68].

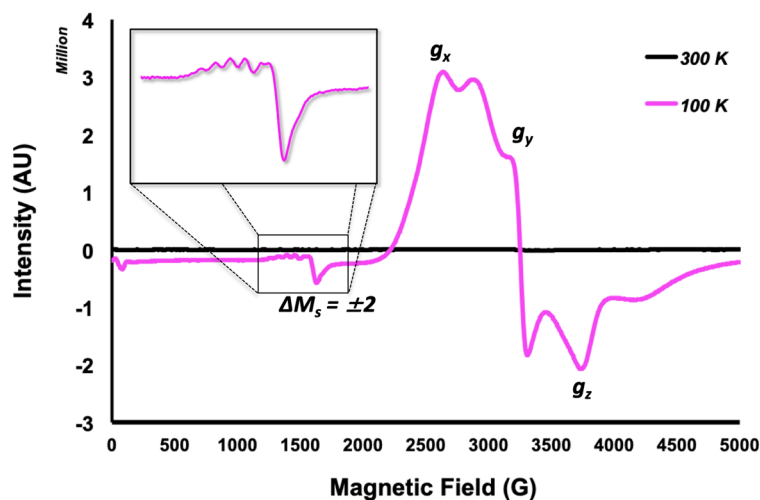


Figure 4. Variable temperature X-band EPR spectra at 300 K (black) and 100 K (purple) of complex 2 recorded in toluene (in solution and frozen glass, respectively).

In conclusion, we have prepared a binuclear copper(II) dipyrriamethyrin complex displaying a unique molecular and electronic structure that differs from bimetallic complexes formed from other hexaphyrin-type expanded porphyrins. These differences are ascribed to the presence of the incorporated pyridine motifs, lack of global aromaticity between the dipyrromethene and pyridine components, and the flexible cavity provided by dipyrriamethyrin. The present work thus serves to highlight how changes in the coordinating motifs within a macrocyclic ligand framework can alter the structural features and chemical properties of multinuclear metal complexes. The information gleaned from this work further advances our design understanding of what is needed to support a specific binuclear transition metal ion-expanded porphyrinoid complexation motifs. It thus sets the stage for further work in what is likely to be a rich subfield lying at the nexus of expanded porphyrin and inorganic coordination chemistry.

3. Materials and Methods

All reagents and solvents were purchased from Sigma Aldrich (Milwaukee, WI, USA) and ACROS Organics (Morris Plains, NJ, USA) and used without further purification unless otherwise noted. Column chromatography was carried out using basic alumina (aluminum oxide, basic, Brockmann 1, 50–200 μm , 60 Å; ACROS Organics (Morris Plains, NJ, USA)). High-resolution mass spectrometric (HRMS) measurements were conducted by Dr. Ian Riddington and co-workers in The University of Texas at Austin Department of Chemistry Mass Spectrometry Facility using an Ion Spec Fourier Transform mass spectrometer (Agilent Technologies 6530 Accurate-Mass Q-TOF LC/MS, 9.4 T, USA). UV-Vis spectra were recorded from 250 to 800 nm using a Varian Cary 5000 spectrophotometer (Agilent, USA) at room temperature. A cell length of 10 mm was used for all UV-Vis spectral studies. Variable temperature (VT) electron paramagnetic resonance (EPR) spectroscopy at X-band (9.5 GHz) was carried out using a Bruker EMX Plus spectrometer (USA). Experimental settings consisted of an amplitude modulation = 10 G and a microwave power = 2 mW. The time constant was set to 20.48 msec with a 40.00 msec conversion time and 160.00 sec sweep time. The resolution in X was set to 4000 and final spectrum were an average of 8 scans. Saturated solutions of **2** in anhydrous toluene were used for the EPR analyses and studied either as a solution or frozen glass as dictated by the choice of measurement temperature.

Synthesis of Binuclear Copper Complex (2). To a scintillation vial charged with a 5 mm PTFE stir bar and dipyrriamethyrin (**1**) [26] (50 mg, 0.061 mmol) was added Cu(OAc)₂ (279 mg, 1.53 mmol, 25 equiv.) and 10 mL of a methanol: CH₂Cl₂ (1:1, *v/v*) mixture. The reaction vessel was capped and stirred at room temperature for 16 h. After this time, the solvent was removed under a stream of nitrogen. The solid obtained in this way was suspended in 5 mL of dichloromethane and filtered through a glass pipette plug of Celite into a clean scintillation vial. The reaction vial was washed first with 2.5 mL of CH₂Cl₂ and again with 5 mL of a dichloromethane: hexanes (1:4, *v/v*) mixture, which were also filtered through the Celite plug. The organics were combined into a 20 mL scintillation vial, diluted with an additional 5 mL of hexanes, and allowed to sit loosely capped in the dark overnight. The resultant material was filtered to yield **2** as a dark purple solid with green metallic luster (44–45 mg, 68–70%). Single crystals suitable for X-ray diffraction analysis were grown by dissolving ca. 10 mg of **2** into 2.5 mL of a CH₂Cl₂: hexanes (1:2, *v/v*) mixture. As noted in the main body of the text, attempts to purify complex **2** *via* silica gel, neutral aluminum oxide, or basic aluminum oxide column chromatography resulted in loss of product on the column or reversion to the free base ligand (**1**).

Supplementary Materials: The following are available online, Figure S1: Photograph of binuclear copper(II) complex **2** (CCDC No. 1984261). Figure S2: Single crystal X-ray diffraction data showing additional coordination of the axial acetate carbonyl oxygen to Cu(II). Scheme S1: Proposed positive allosteric mechanism for the formation of binuclear copper(II) complex **2**. Figure S3: .cif and X-ray crystallographic experimental data. Table S1. Crystal data and structure refinement for **2**. Table S2. Atomic coordinates and equivalent isotropic displacement parameters for **2**. Table S3. Bond lengths and angles for **2**. Table S4. Anisotropic displacement parameters for **2**. Table S5. Hydrogen coordinates and isotropic displacement parameters for **2**. Table S6. Torsion angles for **2**.

Author Contributions: Conceptualization, J.T.B.II and J.L.S.; methodology, J.T.B.II, H.D.R., H.Z., G.D.T., V.M.L., J.H., and A.C.S.; writing—original draft preparation, J.T.B.II and J.L.S.; writing—review and editing, J.T.B.II and J.L.S.; supervision, J.L.S.; funding acquisition, J.L.S. All authors have read and agreed to the published version of the manuscript.

Funding: This research was funded by the US National Science Foundation (grant CHE – 1807152 to J.L.S.) and the Robert A. Welch Foundation (F-0018 to J.L.S.).

Acknowledgments: J.T.B. and H.D.R. would like to thank The University of Texas at Austin for a Scientist in Residence Fellowship. H.D.R. would like to thank The University of Texas at Austin for a Provost’s Graduate Excellence Fellowship.

Conflicts of Interest: The authors declare no conflict of interest

References and Notes

1. Waldron, K.J.; Rutherford, J.C.; Ford, D.; Robinson, N.J. Metalloproteins and Metal Sensing. *Nature* **2009**, *460*, 823–830. [[CrossRef](#)] [[PubMed](#)]
2. Andreini, C.; Bertini, I.; Cavallaro, G.; Holliday, G.L.; Thornton, J.M. Metal ions in biological catalysis: From enzyme databases to general principles. *J. Biol. Inorg. Chem.* **2008**, *13*, 1205–1218. [[CrossRef](#)] [[PubMed](#)]
3. Barnett, J.P.; Scanlan, D.J.; Blindauer, C.A. Protein fractionation and detection for metalloproteomics: Challenges and approaches. *Anal. Bioanal. Chem.* **2012**, *402*, 3311–3322. [[CrossRef](#)] [[PubMed](#)]
4. Valasatava, Y.; Rosato, A.; Furnham, N.; Thornton, J.M.; Andreini, C. To what extent do structural changes in catalytic metal sites affect enzyme function? *J. Inorg. Biochem.* **2018**, *179*, 40–53. [[CrossRef](#)] [[PubMed](#)]
5. Tottey, S.; Waldron, K.J.; Firbank, S.J.; Reale, B.; Bessant, C.; Sato, K.; Cheek, T.R.; Gray, J.; Banfield, M.J.; Dennison, C.; et al. Protein-folding location can regulate manganese-binding versus copper- or zinc-binding. *Nature* **2008**, *455*, 1138–1142. [[CrossRef](#)] [[PubMed](#)]
6. Mirts, E.N.; Bhagi-Damodaran, A.; Liu, Y. Understanding and Modulating Metalloenzymes with Unnatural Amino Acids, Non-Native Metal Ions, and Non-Native Metallocofactors. *Acc. Chem. Res.* **2019**, *52*, 935–944. [[CrossRef](#)]
7. Jeschek, M.; Panke, S.; Ward, T.R. Artificial Metalloenzymes on the Verge of New-to-Nature Metabolism. *Trends Biotechnol.* **2018**, *36*, 60–72. [[CrossRef](#)]
8. Schwizer, F.; Okamoto, Y.; Heinisch, T.; Gu, Y.; Pellizzoni, M.M.; Lebrun, V.; Reuter, R.; Kohler, V.; Lewis, J.C.; Ward, T.R. Artificial Metalloenzymes: Reaction Scope and Optimization Strategies. *Chem. Rev.* **2018**, *118*, 142–231. [[CrossRef](#)]

9. Yu, F.; Cangelosi, V.M.; Zastrow, M.L.; Tegoni, M.; Plegaria, J.S.; Tebo, A.G.; Mocny, C.S.; Ruckthong, L.; Qayyum, H.; Pecoraro, V.L. Protein Design: Toward Functional Metalloenzymes. *Chem. Rev.* **2014**, *114*, 3495–3578. [[CrossRef](#)]
10. Lu, Y.; Yeung, N.; Sieracki, N.; Marshall, N.M. Design of functional metalloproteins. *Nature* **2009**, *460*, 855–862. [[CrossRef](#)]
11. Wieszczycka, K.; Staszak, K. Artificial metalloenzymes as catalysts in non-natural compounds synthesis. *Coord. Chem. Rev.* **2017**, *351*, 160–171. [[CrossRef](#)]
12. Groves, J.T.; Watanabe, Y. Reactive iron porphyrin derivatives related to the catalytic cycles of cytochrome P-450 and peroxidase. Studies of the mechanism of oxygen activation. *J. Am. Chem. Soc.* **1988**, *110*, 8443–8452. [[CrossRef](#)]
13. Joshi, T.; Graham, B.; Spiccia, L. Macrocyclic Metal Complexes for Metalloenzyme Mimicry and Sensor Development. *Acc. Chem. Res.* **2015**, *48*, 2366–2379. [[CrossRef](#)] [[PubMed](#)]
14. Happe, T.; Hemschemeier, A. Metalloprotein mimics – old tools in a new light. *Trends Biotechnol.* **2014**, *32*, 170–176. [[CrossRef](#)]
15. Chen, K.-W.; Yang, F.-A.; Chen, J.-H.; Wang, S.-S.; Tung, J.-Y. A novel bismercury(II) complex of bidentate N²¹, N²²-bridged porphyrin: [(benzamido-κN)phenylmercury-κHg-N²¹, N²²]-meso-tetraphenyl porphyrinato-N²³, N²⁴]phenylmercury(II) toluene solvate. *Polyhedron* **2008**, *27*, 2216–2220. [[CrossRef](#)]
16. Thompson, S.J.; Brennan, M.R.; Lee, S.Y.; Dong, G. Synthesis and applications of rhodium porphyrin complexes. *Chem. Soc. Rev.* **2018**, *47*, 929–981. [[CrossRef](#)]
17. Cullen, D.; Meyer, E.; Srivastava, T.S.; Tsutsui, M. Unusual metalloporphyrins. XIV. Structure of [meso-tetraphenylporphyrinato]bis[tricarbonylrhenium(I)]. *J. Am. Chem. Soc.* **1972**, *94*, 7603–7605. [[CrossRef](#)]
18. Takenaka, A.; Sasada, Y.; Omura, T.; Ogoshi, H.; Yoshida, Z.-I. Crystal structure of μ-octaethylporphyrinato-bis[dicarbonylrhodium(I)]. *J. Chem. Soc. Chem. Commun.* **1973**, 792–793. [[CrossRef](#)]
19. Tsutsui, M.; Hsung, C.P.; Ostfeld, D.; Srivastava, T.S.; Cullen, D.L.; Meyer, E.F., Jr. Unusual Metalloporphyrin Complexes of Rhenium and Technetium. *J. Am. Chem. Soc.* **1975**, *97*, 3952–3965. [[CrossRef](#)]
20. Callot, H.J.; Chevrier, B.; Weiss, R. Sitting-atop Porphyrin Complexes. The Structure of the Bischloromercury(II) complex of N-Tosyamino-octaethylporphyrin. *J. Am. Chem. Soc.* **1979**, *101*, 7729–7730. [[CrossRef](#)]
21. Brothers, P.J. Boron Complexes of Pyrrolyl Ligands. *Inorg. Chem.* **2011**, *50*, 12374–12386. [[CrossRef](#)] [[PubMed](#)]
22. Brothers, P.J. Boron complexes of porphyrins and related polypyrrole ligands: Unexpected chemistry for both boron and the porphyrin. *Chem. Commun.* **2008**, 2090–2102. [[CrossRef](#)] [[PubMed](#)]
23. Sessler, J.L.; Tomat, E. Transition Metal Complexes of Expanded Porphyrins. *Acc. Chem. Res.* **2007**, *40*, 371–379. [[CrossRef](#)] [[PubMed](#)]
24. Alka, A.; Shetti, V.S.; Ravikanth, M. Coordination chemistry of expanded porphyrins. *Coord. Chem. Rev.* **2019**, *401*, 213063. [[CrossRef](#)]
25. Mori, H.; Osuka, A. Bimetal Complexes of 5,20-Bis(5-formyl-2-pyrrolyl)-[26]hexaphyrin(1.1.1.1.1.1) Exhibiting Strong Near-Infrared Region Absorptions. *Chem. Eur. J.* **2015**, *21*, 7007–7011. [[CrossRef](#)]
26. Rath, H.; Aratani, N.; Lim, J.M.; Lee, J.S.; Kim, D.; Shinokubo, H.; Osuka, A. Bis-rhodium hexaphyrins: Metalation of [28]hexaphyrin and a smooth Hückel aromatic-antiaromatic interconversion. *Chem. Commun.* **2009**, 3762–3764. [[CrossRef](#)]
27. Shimoura, K.; Kai, H.; Nakamura, Y.; Hong, Y.; Mori, S.; Miki, K.; Ohe, K.; Notsuka, Y.; Yamaoka, Y.; Ishida, M.; et al. Bis-Metal Complexes of Double N-Confused Dioxohexaphyrins as Potential Near-Infrared-II Photoacoustic Dyes. *J. Am. Chem. Soc.* **2020**, *142*, 4429–4437. [[CrossRef](#)]
28. Sessler, J.L.; Tomat, E.; Mody, T.D.; Lynch, V.M.; Veauthier, J.M.; Mirsaidov, U.; Markert, J.T. A Schiff Base Expanded Porphyrin Macrocyclic Ligand that Acts as a Versatile Binucleating Ligand for Late First-Row Transition Metals. *Inorg. Chem.* **2005**, *44*, 2125–2127. [[CrossRef](#)]
29. Reiter, W.A.; Gerges, A.; Lee, S.; Deffo, T.; Clifford, T.; Danby, A.; Bowman-James, K. Accordion porphyrins: Hybrid models for heme and binuclear monooxygenases. *Coord. Chem. Rev.* **1998**, *174*, 343–359. [[CrossRef](#)]
30. Tomat, E.; Cuesta, L.; Lynch, V.M.; Sessler, J.L. Binuclear Fluoro-Bridged Zinc and Cadmium Complexes of a Schiff Base Expanded Porphyrin: Fluoride Abstraction from the Tetrafluoroborate Anion. *Inorg. Chem.* **2007**, *46*, 6224–6226. [[CrossRef](#)] [[PubMed](#)]
31. Sarma, T.; Panda, P.K. Annulated Isomeric, Expanded, and Contracted Porphyrins. *Chem. Rev.* **2017**, *117*, 2785–2838. [[CrossRef](#)] [[PubMed](#)]

32. Khusnutdinova, D.; Wadsworth, B.L.; Flores, M.; Beiler, A.M.; Cruz, E.A.R.; Zenkov, Y.; Moore, G.F. Electrocatalytic Properties of Binuclear Cu (II) Fused Porphyrins for Hydrogen Evolution. *ACS Catal.* **2018**, *8*, 9888–9898. [[CrossRef](#)]
33. Cuesta, L.; Tomat, E.; Lynch, V.M.; Sessler, J.L. Binuclear organometallic ruthenium complexes of a Schiff base expanded porphyrin. *Chem. Commun.* **2008**, 3744–3746. [[CrossRef](#)] [[PubMed](#)]
34. Montenegro-Pohlhammer, N.; Urzua-Leiva, R.; Paez-Hernandez, D.; Cardenas-Jiron, G. Spin-filter transport and magnetic properties in a binuclear Cu(II) expanded porphyrin based molecular junction. *Dalton Trans.* **2019**, *48*, 8418–8426. [[CrossRef](#)] [[PubMed](#)]
35. Pan, Q.-J.; Shamov, G.A.; Schreckenback, G. Binuclear Uranium(VI) Complexes with a “Pacman” Expanded Porphyrin: Computational Evidence for Highly Unusual Bis-Actinyl Structures. *Chem. Eur. J.* **2010**, *16*, 2282–2290. [[CrossRef](#)] [[PubMed](#)]
36. Arnold, P.L.; Jones, G.M.; Odoh, S.O.; Schreckenbach, G.; Magnani, N.; Love, J.B. Strongly coupled binuclear uranium-oxo complexes from uranyl oxo rearrangement and reductive silylation. *Nat. Chem.* **2012**, *4*, 221–227. [[CrossRef](#)]
37. Setsune, J.-i.; Kawama, M.; Nishinaka, T. Helical binuclear Co(II) complexes of pyriporphyrin analogue for sensing homochiral carboxylic acids. *Tet. Lett.* **2011**, *52*, 1773–1777. [[CrossRef](#)]
38. Vogel, E.; Michels, M.; Zander, L.; Lex, J.; Tuzun, N.S.; Houk, K.N. Spirodiporphyrins- As Binuclear Metal Complexes. *Angew. Chem., Int. Ed.* **2003**, *42*, 2857–2862. [[CrossRef](#)]
39. Samala, S.; Dutta, R.; He, Q.; Park, Y.; Chandra, B.; Lynch, V.M.; Jung, Y.M.; Sessler, J.L.; Lee, C.-H. A robust bis-rhodium(I) complex of π -extended planar, anti-aromatic hexaphyrin[1.0.1.0.1.0]. *Chem. Commun.* **2020**, *56*, 758–761. [[CrossRef](#)]
40. Frensch, L.K.; Propper, K.; John, M.; Demeshko, S.; Bruckner, C.; Meyer, F. Siamese-Twin Porphyrin: A Pyrazole-Based Expanded Porphyrin Providing a Bimetallic Cavity. *Angew. Chem., Int. Ed.* **2011**, *50*, 1420–1424. [[CrossRef](#)]
41. Blusch, L.K.; Craigo, K.E.; Martin-Diaconescu, V.; McQuarters, A.B.; Bill, E.; Dechert, S.; DeBeer, S.; Lehnert, N.; Meyer, F. Hidden Non-Innocence in an Expanded Porphyrin: Electronic Structure of the Siamese-Twin Porphyrin’s Dicopper Complex in Different Oxidation States. *J. Am. Chem. Soc.* **2013**, *135*, 13892–13899. [[CrossRef](#)] [[PubMed](#)]
42. Carre, F.H.; Corriu, R.J.P.; Bolin, G.; Moreau, J.J.E.; Vernhet, C. Aminosilanes in Organic Synthesis. Preparation of New Expanded Porphyrin Ligands and Bimetallic Transition-Metal Complexes. Crystal Structure of Tetrapyrrole Macrocyclic Dirhodium Complex. *Organometallics* **1993**, *12*, 2478–2486. [[CrossRef](#)]
43. Corriu, R.J.P.; Bolin, G.; Moreau, J.J.E.; Vernhet, C. A facile synthesis of new tetrapyrrole macrocyclic derivatives. Formation of bimetallic transition metal complexes. *J. Chem. Soc. Chem. Commun.* **1991**, 211–213. [[CrossRef](#)]
44. Stawski, W.; Kijewska, M.; Pawlicki, M. Multi-cation Coordination in Porphyrinoids. *Chem. Asian J.* **2020**, *15*, 8–20. [[CrossRef](#)] [[PubMed](#)]
45. Kohler, T.; Hodgson, M.C.; Seidel, D.; Veauthier, J.M.; Meyer, S.; Lynch, V.; Boyd, P.D.W.; Brothers, P.J.; Sessler, J.L. Octaethylporphyrin and expanded porphyrin complexes containing BF₂ groups. *Chem. Commun.* **2004**, 1060–1061. [[CrossRef](#)]
46. Weghorn, S.J.; Sessler, J.L.; Lynch, V.; Baumann, T.F.; Sibert, J.W. Bis[(μ -chloro)copper(II)] Amethyrin: A Bimetallic Copper(II) Complex of an Expanded Porphyrin. *Inorg. Chem.* **1996**, *35*, 1089–1090. [[CrossRef](#)]
47. Sessler, J.L.; Melfi, P.J.; Tomat, E.; Lynch, V.M. Copper(II) and oxovanadium(V) complexes of hexaphyrin(1.0.1.0.0.0). *Dalton Trans.* **2007**, 629–632. [[CrossRef](#)]
48. Brewster, J.T., II; Anguera, G.; Moore, M.D.; Dolinar, B.S.; Zafar, H.; Thiabaud, G.D.; Lynch, V.M.; Humphrey, S.M.; Sessler, J.L. Synthesis and Characterization of a Binuclear Copper(II) Naphthoisoamethyrin Complex Displaying Weak Antiferromagnetic Coupling. *Inorg. Chem.* **2017**, *56*, 12665–12669. [[CrossRef](#)]
49. Brewster, J.T., II; He, Q.; Anguera, G.; Moore, M.D.; Ke, X.-S.; Lynch, V.M.; Sessler, J.L. Synthesis and characterization of a dipyrriamethyrin-uranyl complex. *Chem. Commun.* **2017**, *53*, 4981–4984. [[CrossRef](#)]
50. Brewster, J.T., II; Mangel, D.N.; Gaunt, A.J.; Saunders, D.P.; Zafar, H.; Lynch, V.M.; Boreen, M.A.; Garner, M.E.; Goodwin, C.A.P.; Settineri, N.S.; et al. In-Plane Thorium(IV), Uranium(IV), and Neptunium(IV) Expanded Porphyrin Complexes. *J. Am. Chem. Soc.* **2019**, *141*, 17867–17874. [[CrossRef](#)]

51. Bruckner, C.; Zhang, Y.; Rettig, S.J.; Dolphin, D. Synthesis, derivatization and structural characterization of octahedral tris(5-phenyl-4,6-dipyrrinato) complexes of cobalt(III) and iron(III). *Inorg. Chim. Acta.* **1997**, *263*, 279–286. [[CrossRef](#)]
52. Halper, S.R.; Cohen, S.M. Synthesis, Structure, and Spectroscopy of Phenylacetylene Rods Incorporating *meso*-Substituted Dipyrrin Ligands. *Chem. Eur. J.* **2003**, *9*, 4661–4669. [[CrossRef](#)]
53. Halper, S.R.; Malachowski, M.R.; Delaney, H.M.; Cohen, S.M. Heteroleptic Copper Dipyromethene Complexes: Synthesis, Structure, and Coordination Polymers. *Inorg. Chem.* **2004**, *43*, 1242–1249. [[CrossRef](#)] [[PubMed](#)]
54. Liu, X.; Nan, H.; Sun, W.; Zhang, Q.; Zhan, M.; Zou, L.; Xie, Z.; Li, X.; Lu, C.; Cheng, Y. Synthesis and characterisation of neutral mononuclear cuprous complexes based on dipyrin derivatives and phosphine mixed-ligands. *Dalton Trans.* **2012**, *41*, 10199–10210. [[CrossRef](#)] [[PubMed](#)]
55. Sessler, J.L.; Tomat, E.; Lynch, V.M. Positive Homotropic Allosteric Binding of a Silver(I) Cations in a Schiff Base Oligopyrrolic Macrocycle. *J. Am. Chem. Soc.* **2006**, *128*, 4184–4185. [[CrossRef](#)] [[PubMed](#)]
56. Setsune, J.-I.; Watanabe, K. Cryptand-like Porphyrinoid Assembled with Three Dipyrpyridine Chains: Synthesis, Structure, and Homotropic Positive Allosteric Binding of Carboxylic Acids. *J. Am. Chem. Soc.* **2008**, *8*, 2404–2405. [[CrossRef](#)]
57. Macquet, J.P.; Millard, M.M.; Theophanides, T. X-Ray Photoelectron Spectroscopy of Porphyrins. *J. Am. Chem. Soc.* **1978**, *100*, 4741–4746. [[CrossRef](#)]
58. Shen, Y.; Ryde, U. The structure of sitting-atop complexes of metalloporphyrins studied by theoretical methods. *J. Inorg. Biochem.* **2004**, *98*, 878–895. [[CrossRef](#)]
59. De Luca, G.; Romeo, A.; Scolaro, L.M.; Ricciardi, G.; Rosa, A. Sitting-Atop Metallo-Porphyrin Complexes: Experimental and Theoretical Investigations on Such Elusive Species. *Inorg. Chem.* **2009**, *48*, 8493–8507. [[CrossRef](#)]
60. Duedal, T.; Nielsen, K.A.; Olsen, G.; Rasmussen, C.B.G.; Kongsted, J.; Levillain, E.; Breton, T.; Miyazaki, E.; Takimiya, K.; Bähring, S.; et al. Very Strong Binding for a Neutral Calix[4]pyrrole Receptor Displaying Positive Allosteric Binding. *J. Org. Chem.* **2017**, *82*, 2123–2128. [[CrossRef](#)]
61. Gorelsky, S.I.; Lapointe, D.; Fagnou, K. Analysis of the Concerted Metalation-Deprotonation Mechanism in Palladium-Catalyzed Direct Arylation Across a Broad Range of Aromatic Substrates. *J. Am. Chem. Soc.* **2008**, *130*, 10848–10849. [[CrossRef](#)] [[PubMed](#)]
62. Rao, W.-H.; Shi, B.-F. Recent advances in copper-mediated chelation-assisted functionalization of unactivated C-H bonds. *Org. Chem. Front.* **2016**, *3*, 1028–1047. [[CrossRef](#)]
63. Lapointe, D.; Fagnou, K. Overview of the Mechanistic Work on the Concerted Metallation-Deprotonation Pathway. *Chem. Lett.* **2010**, *39*, 1118–1126. [[CrossRef](#)]
64. Addison, A.W.; Rao, T.N.; Reedijk, J.; van Rijn, J.; Verschoor, G.C. Synthesis, structure, and spectroscopic properties of copper(II) compounds containing nitrogen-sulphur donor ligands; the crystal and molecular structure of aqua[1,7-bis(*N*-methylbenzimidazol-2'-yl)-2,6-dithiaheptane]copper(II) perchlorate. *J. Chem. Soc. Dalton Trans.* **1984**, *7*, 1349–1356. [[CrossRef](#)]
65. The α value was calculated using the smallest N-Cu-O angle. The β -value was calculated using the axial N-Cu-N angle. τ was calculated as $(\beta-\alpha)/60$.
66. Halcrow, M.A. Jahn-Teller Distortions in Transition Metal Compounds and Their Importance in Functional Molecular and Inorganic Materials. *Chem. Soc. Rev.* **2013**, *42*, 1784–1795. [[CrossRef](#)]
67. Wang, R.; Brugh, A.M.; Rawson, J.; Therien, M.J.; Forbes, M.D.E. Alkyne-Bridged Multi[Copper(II) Porphyrin] Structures: Nuances of Orbital Symmetry in Long Range, Through-Bond Mediated Isotropic Spin Exchange Interactions. *J. Am. Chem. Soc.* **2017**, *139*, 9759–9762. [[CrossRef](#)]
68. Selyutin, G.E.; Shklyayev, A.A.; Shul'ga, A.M. EPR Spectral Study of the Structure of Dimers of Copper(II) Porphyrin and Phthalocyanine Complexes. *Russ. Chem. Bull.* **1985**, *34*, 1218–1223. [[CrossRef](#)]

Sample Availability: Not available.



© 2020 by the authors. Licensee MDPI, Basel, Switzerland. This article is an open access article distributed under the terms and conditions of the Creative Commons Attribution (CC BY) license (<http://creativecommons.org/licenses/by/4.0/>).